NIH Public Access
Author Manuscript
Angew Chem Int Ed Engl. Author manuscript; available in PMC 2011 January 11.

Published in final edited form as:
Angew Chem Int Ed Engl. 2010 October 25; 49(44): 8177–8180. doi:10.1002/anie.201004429.

Probing a Homoleptic PbS_3 Coordination Environment in a Designed Peptide Using ^{207}Pb NMR Spectroscopy: Implications for Understanding the Molecular Basis of Lead Toxicity**

Dr. Kosh P. Neupane and **Prof. Dr. Vincent L. Pecoraro***
Department of Chemistry, University of Michigan, Ann Arbor, MI 48109 (USA)

Keywords

lead; metalloproteins; NMR spectroscopy; proteins; toxicology

Lead is a ubiquitous environmental contaminant; nearly 5% of American children are affected by lead poisoning (a blood lead level (BLL) of 10 $\mu g dL^{-1}$ or higher).[1] Even lower BLLs have been shown to cause many subtle health effects in children. Lead, which is found in paint and soil, causes toxicity by several possible mechanisms. Pb^{2+} interacts with several zinc enzymes or proteins (such as carbonic anhydrase, acetylcholine esterase, Cys_2His_2 "zinc-finger" proteins, and acid phophatases)[2,3] and calcium ion binding proteins (calmodulin, calbindin, and troponin C).[4] Inhibition of protein function is induced by alternative coordination number and structural preferences.[5,6] Pb^{2+} is a chemically interesting toxin in that it can replace calcium and sometimes zinc in "hard" active sites that are oxygen/nitrogen rich; it can also attack softer ligands, such as all-sulfur-containing zinc ion coordination sites. Among the sulfur-rich targets for Pb^{2+} are glutathione and metallothioneines, which cause perturbations of essential metal ion homeostasis.

Aminolevulinic acid dehydratase (ALAD), a zinc-dependent enzyme, is inhibited by a femtomolar concentrations of Pb^{2+}.[2] ALAD is found in yeast and mammals and is involved in the second step of heme biosynthesis. Pb^{2+}-poisoned ALAD blocks the synthesis of hemoglobin, causing anemia in mammals. Furthermore, toxic levels of aminolevulinic acid can result. The crystal structure of ALAD contains an unusual $Zn(Cys)_3H_2O$ site, where Zn^{2+} is substituted by Pb^{2+} in a trigonal pyramidal geometry.[7] The high affinity of Pb^{2+} to cysteine thiolates is presumably due to the high enthalpy of Pb–S bond formation and the preferred PbS_3 coordination geometry in thiolate-rich sites of proteins.[8] A number of peptides[9–11] and small-molecule synthetic models[12] have been used to understand the chemistry of the Pb^{II}-poisoned ALAD. UV/Vis and EXAFS studies on the metalloregulatory protein Pb-PbrR691 and Pb^{2+} model compounds reveal that Pb^{2+} binds in a PbS_3 environment.[13]

Heteronuclear magnetic resonance spectroscopy with nuclei such as ^{43}Ca, ^{113}Cd, and ^{199}Hg has been a powerful tool for studying the active site structures of metalloenzymes and their model compounds.[14–21] Similarly, lead provides an NMR active nucleus (^{207}Pb, nuclear spin $I = 1/2$) with a natural abundance of 22.6% and a relatively good receptivity (11.7 times

**V.L.P. thanks the National Institute of Health for support of this research (R01 ES0 12236).

Fax: (+1)734-936-7628, vlpec@umich.edu.

NIH-PA Author Manuscript
NIH-PA Author Manuscript
NIH-PA Author Manuscript

NIH-PA Author Manuscript

NIH-PA Author Manuscript

NIH-PA Author Manuscript

higher than that of ^{13}C).[22] However, owing to the wide chemical shift range (over 16000 ppm), the use of ^{207}Pb NMR spectroscopy is non-trivial.[8,22–24]

Recently, Vogel and co-workers utilized ^{207}Pb NMR spectroscopy (using isotopically enriched ^{207}Pb) to study Pb^{2+} binding to the Ca^{2+} site of calcium-binding proteins, including calmodulin (CaM).[25] To our knowledge, this is the sole example of ^{207}Pb NMR as a probe in metalloproteins. Of great importance, there are no reported ^{207}Pb spectra for sulfur-rich metalloproteins. A number of small synthetic molecules with or without mixed O, S, and N donor ligands (for example S_2O_2, S_2N_2, N_2O_4, N_3O_3, N_4, N_6) have been characterized using this technique.[22–24,26–28] The ^{207}Pb NMR signal for the thiol-rich binding sites should be shifted further downfield than that of oxygen- and nitrogen-rich calcium-binding sites. Thus, we can distinguish PbS_3 versus PbS_3O coordination environments very easily by using ^{207}Pb NMR.[22] The coordination number and geometry of the Pb^{2+} ion can also be examined.[29] Dean, Payne, Christou, and their co-workers have synthesized $[Ph_4As][Pb(SPh)_3]$ and characterized complexes in non-aqueous media using ^{207}Pb NMR spectroscopy.[30–32] Despite these studies, no significant advancement of ^{207}Pb NMR has been accomplished to explore the thiolate-rich proteins scaffolds. Herein, we present the ^{207}Pb NMR for a physiologically relevant coordination environment of thiolate-rich metallopeptides in the preferred homoleptic trigonal pyramidal geometry for Pb^{II} ions by utilizing three-strand coiled-coil peptides. To our knowledge, this is the first report of ^{207}Pb NMR spectroscopy used in a Cys_3 motif that can be a direct probe for the thiol-rich metalloenzymes, such as ALAD, which are directly implicated in human lead poisoning.

We have utilized new three-strand coiled-coil (3-SCC) peptides (CoilSer and TRI family) to obtain insight into how toxic metals, such as Hg^{2+}, As^{3+}, Cd^{2+}, and Pb^{2+}, bind in thiol-rich sites of metalloenzymes.[19–21,33–38] These α-helical peptide families have heptad repeats of seven amino acid residues that contain hydrophobic leucine residues in the **a** (first) and **d** (fourth) positions (Table 1).[39] The resultant 3-SCC has all of the hydrophobic leucine residues packed on the interior of the 3-SCC and hydrophilic residues (*e* and *g*) on the exterior, forming salt bridges that stabilize the coiled coil. A metal binding site can be created by the substitution of a leucine by cysteine in the **a** or **d** positions of the heptad repeat unit to give a metal binding site within the hydrophobic core of the peptide trimer.[35,39] The sulfur atoms in an **a** site are oriented towards the interior of the coiled coil and preorganized for metal binding, whereas the sulfur atoms in a **d** site point away from the interior towards the helical interface, creating a relatively larger cavity (Figure 1). Metal ions such as Cd^{2+}, Hg^{2+}, and As^{3+} are preferentially bound to the **a** site, whereas larger metal ions such as Pb^{2+} prefer the **d** site.[40]

The use of these well-defined peptides provides several advantages for detecting the ^{207}Pb signal in an all-thiolate (homoleptic) environment that mimics ALAD. In contrast to small organic lead thiolate complexes, the designed peptides are highly soluble and stable in water. Therefore, ^{207}Pb NMR studies at relatively high concentrations (10–12 mM) and physiological pH is successful without peptide aggregation or $Pb(OH)_2$ precipitation. Similar preparations were unsuccessful for cysteine, which was due to the precipitation of a $PbCys_3$ complex that can only be dissolved at high pH (>12). Thus, a solely PbS_3 coordination environment cannot be attained by cysteine at physiological pH.

Binding studies of Pb^{2+} to **TRI**L12C and **TRI**L16C were previously monitored by UV/Vis, EXAFS, and CD spectroscopy[35] and shown to have high affinity ($>10^8 M^{-1}$) with the peptides studied herein. The presence of a characteristic ligand-to-metal charge-transfer (LMCT) band at about 345 nm ($\varepsilon \approx 3500 Lmol^{-1}cm^{-1}$) is indicative of PbS_3 in a trigonal pyramidal geometry. Recent EXAFS studies by Matzapetakis et al. identified a three-coordinate Pb^{2+} site in $Pb(\mathbf{TRI}L16C)_3^-$ with Pb–S scatters at 2.63 Å. Similar results have

NIH-PA Author Manuscript

NIH-PA Author Manuscript

NIH-PA Author Manuscript

been reported by Giedroc and co-workers for the preference of Pb^{2+} for a PbS_3 coordination environment in the metalloregulatory protein CadC.[41,42] This data compares well with Pb–S scatters found for the lead-inhibited active site of ALAD. Therefore, the metallopeptides described herein are in close approximation to the Pb^{2+}-inhibited active site of ALAD and related lead-binding proteins.

The natural-abundance ^{207}Pb NMR spectra of all of the metal-lopeptides with a single binding site had a single lead signal at 5500–5800 ppm with broad linewidths (15–25 pm) (Figure 2). Similar broad signals have been reported in protein NMR studies with ^{199}Hg and ^{205}Tl, which may be due to nuclear relaxation by chemical shift anisotropy (CSA).[43,44] The peptides with a **d** metal binding site have downfield chemical shifts relative to those of the **a** site peptides. Several interesting trends can be extracted from these data: similar chemical shifts for the peptides having a **d** site are seen independent of the length of the peptide or the intrinsic stability of the aggregate, Pb-(**Baby**L12C)$_3^-$ (δ = 5786 ppm, $w_{1/2}$ = 20 ppm) and Pb-(**CS**L12C)$_3^-$ (δ = 5814 ppm, $w_{1/2}$ = 18 ppm). These chemical shifts are similar to the previously reported trigonal pyramidal PbS_3 structure of a small synthetic organic compound $[Ph_4As][Pb(SPh)_3]$ (δ = 5828 ppm).[31] The possibility of formation of nitrogen- or oxygen-bound species can be ruled out as a distinct upfield chemical shift has been observed for mixed-donor ligand types (PbN_2S, δ = 5318 ppm; PbS_2O_2, δ = 4100–4500 ppm).[8,24,26] Therefore, the observed ^{207}Pb signal can be confidently assigned to the formation of a PbS_3 coordination environment.

An upfield chemical shift of approximately 200 ppm was observed when a lead-binding site was created in the **a** site peptide (Pb(**CS**L16C)$_3^-$; δ = 5612 ppm, $w_{1/2}$ = 18 ppm). Furthermore, substitution of a sterically less-demanding amino acid residue above the **a** metal binding site leads to a 55–60 ppm further upfield shift (Pb(**CS**L12AL16C)$_3^-$; δ = 5555 ppm, $w_{1/2}$ = 25 ppm). We conclude that ^{207}Pb NMR spectroscopy is sufficiently sensitive to distinguish between two similar trigonal pyramidal PbS_3 centers based on the **a** versus **d** substitution pattern of the peptide. Furthermore, the upfield shift in the Pb(**CS**L12AL16C)$_3^-$ suggests that the additional space provided above the PbS_3 plane by the alanine accommodates the bulky Pb^{2+} lone pair within the helical assembly better. A similar rationale can be applied to the longer Pb_2(**Grand**L12AL16L26C)$_3^{2-}$, in which the leucine layer above the **a** site is substituted by alanine and leucines at the 16th (**a**) and 26th (**d**) sites are replaced with cysteines, creating two Pb^{2+} binding sites. The **d** site has a ^{207}Pb NMR signal at δ = 5796 ppm (Figure 2e; $w_{1/2}$ = 17 ppm); this value is between the signal obtained for Pb(**Baby**L12C)$_3^-$ and Pb(**CS**L12C)$_3^-$, but clearly in the region of **d** cysteine ligands. A ^{207}Pb peak at 5538 ppm ($w_{1/2}$ = 18 ppm) is assigned to the **a** site with a hole oriented towards the N terminus, which compares well with the value obtained for Pb(**CS**L12AL16C)$_3^-$. These data illustrate that ^{207}Pb NMR is sufficiently sensitive to discriminate complexation of Pb^{2+} in these similar yet non-identical sites. Furthermore, the simultaneous observation of both peaks and the relatively narrow linewidths suggest that the Pb^{2+} ions are in slow exchange on the NMR timescale.

Interestingly, the addition of one equivalent of $Pb(NO_3)_2$ into **Grand**L12AL16L26C gives a ^{207}Pb signal at the **a** site region only (δ = 5546 ppm, $w_{1/2}$ = 19 ppm), indicating a selective binding of Pb^{2+} to the **a** site with a hole above (Figure 2f). This observation is in contrast to the previously reported **a** versus **d** preference for Pb^{2+} complexation. The inversion of selectivity is a consequence of the added space made available by substituting alanine for leucine. The steriochemically active lone pair of Pb^{2+} no longer clashes with the alkyl side chain of leucine and can now be accommodated within the generated cavity, leading to a higher thermodynamic stability of lead binding. It has been shown that Cd^{2+}, which forms a mixture of three- (CdS_3) and four-coordinate ($CdS_3(H_2O)$) structures with **TRI**L16C,

NIH-PA Author Manuscript

NIH-PA Author Manuscript

NIH-PA Author Manuscript

becomes fully four-coordinate, using an exogenous water ligand, when space is made available above the metal by the same leucine to alanine substitution in **TRI**L12AL16C.[46]

These results provide experimental confirmation of the importance of the lone pair on the selectivity of Pb^{2+} for sulfur sites in proteins such as PbrR691 and ALAD (in which Pb^{2+} displaces Zn^{2+} from three cysteines and one exogeneous water rather than the five-coordinate zinc binding site with nitrogen and oxygen atoms as ligands). These data suggest that there will be a significant preference for Pb^{2+} to be sequestered into an environment that provides sufficient space to accommodate the large lone pair of this ion. Such a situation exists when Pb^{2+} displaces Zn^{2+} in ALAD.

Despite the fact that lead-substituted ALAD is strongly implicated in lead toxicity, to date there have been no examples of biomolecules or model compounds that have exhibited a ^{207}Pb NMR spectrum for a PbS_3 center in aqueous solution at physiological pH. Our ability to detect such a chromophore using natural-abundance isotope levels, to illustrate the sensitivity of the chemical shift range and to demonstrate how slight amino acid sequence changes affect lead binding to a protein are significant advances for understanding the biochemistry of human lead poisoning. Our data also indicate that Pb^{2+} exchange between homoleptic thiolate sites is slow on the NMR timescale. Most importantly, we have demonstrated that high-quality spectra do not require expensive enriched ^{207}Pb, but can be obtained using natural-abundance lead salts. We hope that ^{207}Pb NMR spectroscopy may now be useful to identify and characterize proteins associated with lead toxicity directly from human samples if a sufficiently concentrated sample can be obtained.

Experimental Section

Peptide synthesis and purification

All of the peptides were synthesized on an Applied Biosystems 433A peptide synthesizer by using standard Fmoc/*t*Bu-based protection strategies on Rink Amide MBHA resin (0.25 mmol scale) with HBTU/HOBt/DIEPA coupling methods.[47] The peptides were then cleaved from the resin either using a mixture of 95% trifluoroacetic acid (TFA), 2.5% ethanedithiol, and 2.5% triisopropyl silane or a mixture of 90% TFA, 5% thioanisole, 3% ethanedithiol, and 2% anisole. The cleaved peptide solutions were filtered and then evaporated under a dry N_2 flow to give a glassy film. The white film was washed with ice-cold diethyl ether (peroxide free) to obtain a crude peptide powder. The peptides were dissolved in 10% acetic acid, lyophilized, and subsequently purified by reverse-phase HPLC (Waters 600 with Vydac protein and peptide C-18 column; solvent A: 0.1% TFA in H_2O; solvent B: 0.1% TFA in acetonitrile/H_2O (9:1); linear gradient 20–80% of solvent B over 30 min; flow rate: 10 mL min^{-1}). The identity and purity of the purified peptides was confirmed by electrospray mass spectrometry (Waters) in positive-ion mode and by analytical HPLC. The purity of peptides was more than 95%. All of the peptides studied herein were N-terminally acetylated and C-terminally amidated. A list of the peptides synthesized with their sequences is given in Table 1.

Natural abundance ^{207}Pb NMR spectroscopy

NMR samples (10–12 mM) were prepared under a nitrogen atmosphere by dissolving of pure and dried peptide (70–80 mg) in D_2O/H_2O (15%, 400–500 μL; degassed). The peptide concentration was determined by Ellman's test.[48] Calculated amounts of 250 mM $Pb(NO_3)_2$ (natural abundance) stock solution was added to the peptide solution and the pH was adjusted by the slow addition of a small aliquot of KOH/15% D_2O until the pH reached 7.35 ± 0.05. All of the ^{207}Pb NMR spectra were recorded at a frequency of 104.435 MHz on a Varian 500 MHz NMR spectrometer at room temperature (25°C) using 60° pulses, a 20 ms relaxation delay, and a 20 ms acquisition time. Initially, a large spectral width of 300 KHz

NIH-PA Author Manuscript

NIH-PA Author Manuscript

NIH-PA Author Manuscript

was used to find the position of the peak. Once the peak position was found, the spectral window was reduced to about 166 KHz. However, the chemical shift difference was not observed when the spectral window was about 300 KHz (3000 ppm), 166 KHz (1500 ppm), or 50 KHz (500 ppm). A linear prediction was performed to remove the noise, and the real FID was determined before the data processing. After zero-filling, the data (128 K data points) were processed with an exponential line broadening of 200–250 Hz using the software MestRe-C.[49] The ^{207}Pb NMR chemical shifts are reported downfield from tetramethyllead (δ = 0 ppm; toluene) using 1.0M $Pb(NO_3)_2$ salt (natural) as an external standard (δ = −2990 ppm, D_2O, 25 °C; relative to $PbMe_4$).

References

1. Lanphear BP. Science 1998;281:1617–1618. [PubMed: 9767027]
2. Simons TJB. Eur J Biochem 1995;234:178–183. [PubMed: 8529638]
3. Zawia NH, Crumpton T, Brydie M, Reddy GR, Razmiafshari M. Neurotoxicology 2000;21:1069–1080. [PubMed: 11233753]
4. Simons TJB. Neurotoxicology 1993;14:77–85. [PubMed: 8247414]
5. Razmiafshari M, Zawia NH. Toxicol Appl Pharmacol 2000;166:1–12. [PubMed: 10873713]
6. Zawia NH, Sharan R, Brydie M, Oyama T, Crumpton T. Dev Brain Res 1999;107:291–298. [PubMed: 9593950]
7. Erskine PT, Senior N, Awan S, Lambert R, Lewis G, Tickle IJ, Sarwar M, Spencer P, Thomas P, Warren MJ, Shoolingin-Jordan PM, Wood SP, Cooper JB. Nat Struct Biol 1997;4:1025–1031. [PubMed: 9406553]
8. Andersen RJ, diTargiani RC, Hancock RD, Stern CL, Goldberg DP, Godwin HA. Inorg Chem 2006;45:6574–6576. [PubMed: 16903704]
9. Payne JC, ter Horst MA, Godwin HA. J Am Chem Soc 1999;121:6850–6855.
10. Godwin HA. Curr Opin Chem Biol 2001;5:223–227. [PubMed: 11282351]
11. Magyar JS, Weng TC, Stern CM, Dye DF, Rous BW, Payne JC, Bridgewater BM, Mijovilovich A, Parkin G, Zaleski JM, Penner-Hahn JE, Godwin HA. J Am Chem Soc 2005;127:9495–9505. [PubMed: 15984876]
12. Bridgewater BM, Parkin G. J Am Chem Soc 2000;122:7140–7141.
13. Chen PR, He C. Curr Opin Chem Biol 2008;12:214–221. [PubMed: 18258210]
14. Armitage IM, Pajer RT, Uiterkamp AJMS, Chlebowski JF, Coleman JE. J Am Chem Soc 1976;98:5710–5712. [PubMed: 821988]
15. Armitage IM, Uiterkamp AJMS, Chlebowski JF, Coleman JE. J Magn Reson 1978;29:375–392.
16. Forsen S, Johansson C, Linse S. Methods Enzymol 1993;227:107–118. [PubMed: 8255223]
17. Ellis PD. Science 1983;221:1141–1146. [PubMed: 17811505]
18. Summers MF. Coord Chem Rev 1988;86:43–134.
19. Dieckmann GR, McRorie DK, Tierney DL, Utschig LM, Singer CP, Ohalloran TV, PennerHahn JE, DeGrado WF, Pecoraro VL. J Am Chem Soc 1997;119:6195–6196.
20. Matzapetakis M, Farrer BT, Weng TC, Hemmingsen L, Penner-Hahn JE, Pecoraro VL. J Am Chem Soc 2002;124:8042–8054. [PubMed: 12095348]
21. Utschig LM, Wright JG, Dieckmann G, Pecoraro VL, O'Halloran TV. Inorg Chem 1995;34:2497–2498.
22. Wrackmeyer B, Horchler K. Annu Rep NMR Spectrosc 1990;22:249–306.
23. Claudio ES, ter Horst MA, Forde CE, Stern CL, Zart MK, Godwin HA. Inorg Chem 2000;39:1391–1397. [PubMed: 12526441]
24. Rupprecht S, Franklin SJ, Raymond KN. Inorg Chim Acta 1995;235:185–194.
25. Aramini JM, Hiraoki T, Yazawa M, Yuan T, Zhang MJ, Vogel HJ. J Biol Inorg Chem 1996;1:39–48.
26. Rupprecht S, Langemann K, Lugger T, McCormick JM, Raymond KN. Inorg Chim Acta 1996;243:79–90.

NIH-PA Author Manuscript

NIH-PA Author Manuscript

NIH-PA Author Manuscript

27. Pedrido R, Bermejo MR, Romero MJ, Vazquez M, Gonzalez-Noya AM, Maneiro M, Rodriguez MJ, Fernandez MI. Dalton Trans 2005:572–579. [PubMed: 15672203]
28. Reger DL, Ding Y, Rheingold AL, Ostrander RL. Inorg Chem 1994;33:4226–4230.
29. Claudio ES, Godwin HA, Magyar JS. Prog Inorg Chem 2003;51:1–144.
30. Arsenault JJI, Dean PAW. Can J Chem 1983;61:1516–1523.
31. Dean PW, Vittal JJ, Payne NC. Inorg Chem 1984;23:4232–4236.
32. Christou G, Folting K, Huffman JC. Polyhedron 1984;3:1247–1253.
33. Farrer BT, McClure CP, Penner-Hahn JE, Pecoraro VL. Inorg Chem 2000;39:5422–5423. [PubMed: 11154553]
34. Iranzo O, Ghosh D, Pecoraro VL. Inorg Chem 2006;45:9959–9973. [PubMed: 17140192]
35. Matzapetakis M, Ghosh D, Weng TC, Penner-Hahn JE, Pecoraro VL. J Biol Inorg Chem 2006;11:876–890. [PubMed: 16855818]
36. Dieckmann GR, McRorie DK, Lear JD, Sharp KA, DeGrado WF, Pecoraro VL. J Mol Biol 1998;280:897–912. [PubMed: 9671558]
37. Farrer BT, Pecoraro VL. Proc Natl Acad Sci USA 2003;100:3760–3765. [PubMed: 12552128]
38. Ghosh D, Pecoraro VL. Inorg Chem 2004;43:7902–7915. [PubMed: 15578824]
39. Peacock AFA, Iranzo O, Pecoraro VL. Dalton Trans 2009:2271–2280. [PubMed: 19290357]
40. Matzapetakis, M. University of Michigan. Ann Arbor: 2004.
41. Busenlehner LS, Cosper NJ, Scott RA, Rosen BP, Wong MD, Giedroc DP. Biochemistry 2001;40:4426–4436. [PubMed: 11284699]
42. Busenlehner LS, Weng TC, Penner-Hahn JE, Giedroc DP. J Mol Biol 2002;319:685–701. [PubMed: 12054863]
43. Utschig LM, Bryson JW, O'Halloran TV. Science 1995;268:380–385. [PubMed: 7716541]
44. Aramini JM, Krygsman PH, Vogel HJ. Biochemistry 1994;33:3304–3311. [PubMed: 8136366]
45. Peacock AFA, Stuckey JA, Pecoraro VL. Angew Chem 2009;121:7507–7510.Angew Chem Int Ed 2009;48:7371–7374.
46. Iranzo O, Jakusch T, Lee KH, Hemmingsen L, Pecoraro VL. Chem Eur J 2009;15:3761–3772.
47. Chan, WC.; White, PD. Fmoc Solid-Phase Peptide Synthesis: A Practical Approach. Oxford University Press; New York: 2000.
48. Ellman GL. Arch Biochem Biophys 1958;74:443–450. [PubMed: 13534673]
49. Cobas, C.; Cruces, J.; Sardina, FJ. MestRe-C version 2.3. Universidad de Santiago de Compostela; Spain: 2000.

NIH-PA Author Manuscript

NIH-PA Author Manuscript

NIH-PA Author Manuscript

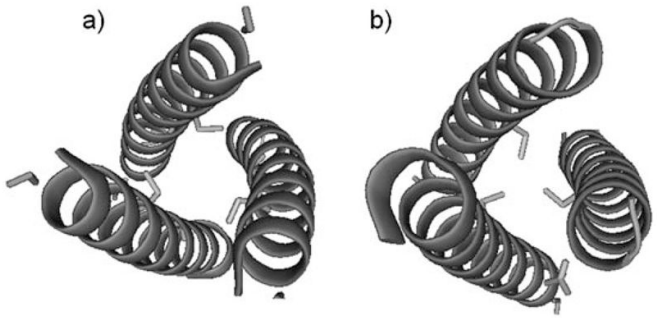

Figure 1.
Pymol representation showing the orientation of cysteine residues. a) **CoilSer**L12C, **d** site; b) **CoilSer**L16C, **a** site. Cysteine side chains are shown as sticks and peptide α helices are shown as coils. PDB code: 3H5F.[45]

NIH-PA Author Manuscript
NIH-PA Author Manuscript
NIH-PA Author Manuscript

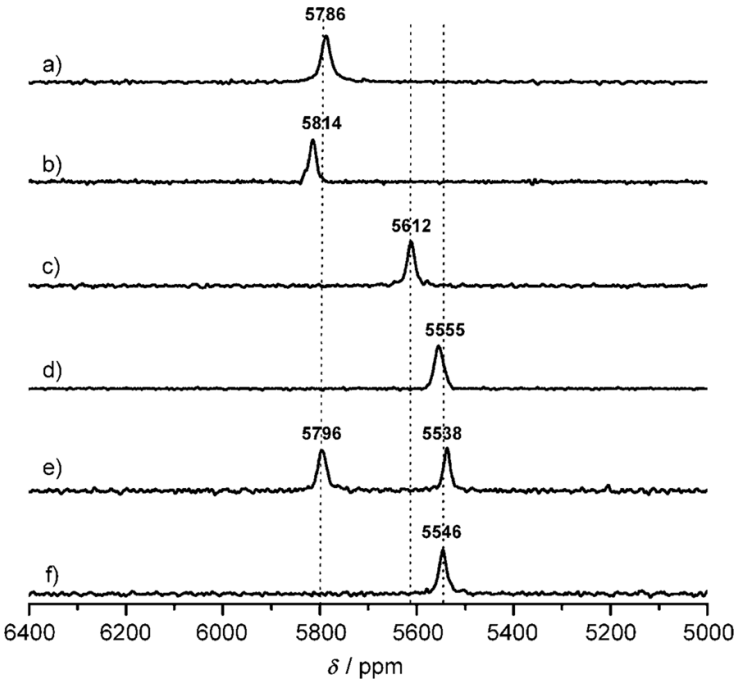

Figure 2.

Natural-abundance ^{207}Pb NMR spectra (104.435 MHz) of Pb^{II}-bound three-strand coiled-coil peptides (10–12 mM): a) Pb-(**Baby**L12C)$_3^-$, b) Pb(**CS**L12C)$_3^-$, c) Pb(**CS**L16C)$_3^-$, d) Pb(**CS**L12AL16C)$_3^-$, e) Pb_2(**Grand**L12AL16L26C)$_3^{2-}$, f) Pb(**Grand-**L12AL16L26C)$_3^-$. All spectra were recorded for 10–12 h using natural-abundance $Pb(NO_3)_2$, (^{207}Pb = 22.6%), pH 7.35 ± 0.05, at 25°C.

NIH-PA Author Manuscript

NIH-PA Author Manuscript

NIH-PA Author Manuscript

Table 1

Sequence and name of the peptides used in this study.

Peptides	**Sequence**
	abcdefg abcdefg abcdefg abcdefg
CSL12C	Ac-E WEALEKK LAA**C**ESK LQALEKK LEALEHG-NH_2
CSL16C	Ac-E WEALEKK LAALESK **C**QALEKK LEALEHG-NH_2
CSL12AL16C	Ac-E WEALEKK LAA**A**ESK **C**QALEKK LEALEHG-NH_2
BabyL12C	Ac-G LKALEEK LKA**C**EEK LKALEEK G-NH_2
GrandL12AL16CL26C	Ac-G LKALEEK LKA**A**EEK **C**KALEEK LKA**C**EEK LKALEEK G-NH_2